

CHROMOSPHERICALLY ACTIVE LOW-MASS CLOSE BINARY: KIC 9761199

E. YOLDAŞ¹ and H. A. DAL^{1,2}

Draft version: November 8, 2016

RESUMEN

Favor de proporcionar un resumen en español. If you are unable to translate your abstract into Spanish, the editors will do it for you.

ABSTRACT

In this study, we present the results obtained from KIC 9761199's the photometrical data acquired by the Kepler Mission. The light curve of the system, the sinusoidal variation out-of-eclipses and instant-short term flare events in the entire light curves were analyzed. The temperature of the secondary component was found to be 3891 ± 1 K, while the mass ratio of the components (q) was found to be 0.69 ± 0.01 , and the orbital inclination (i) was computed as $77^\circ.4 \pm 0^\circ.1$. The sinusoidal variation is caused by the stellar spots of two active regions separated by about 180° longitudinally located around the latitudes of $+47^\circ$ and $+30^\circ$. In addition, 94 flares were detected and their parameters were computed. The OPEA model was derived for these flares and its parameters were computed. The *Plateau* value as saturation level for the active component was found to be 1.951 ± 0.069 s, while the *half-life* value was found to be 1014 s. The flare frequency N_1 was found to be $0.01351 h^{-1}$, while the flare frequency N_2 was found to be 0.00006. Maximum flare rise time (T_r) was found to be 1118.098 s, while maximum flare total time (T_t) was found to be 6767.72 s. Comparing its analogue it is seen that the chromospheric activity level of KIC 9761199, which is a low-mass close binary system according to the light curve analyses, is an expected level according to the $(B - V)$ color index of $1^m.303$ for the active component.

Key Words: techniques: photometric — methods: data analysis — stars: binaries: eclipsing — stars: low-mass — stars: flare — stars: individual: KIC 9761199

1. INTRODUCTION

It is well known for several decades that the population rate of red dwarfs in our Galaxy is about 65%, while seventy-five percent of them show flare activity. The stars exhibiting flare activity are known as UV Ceti type stars (Rodonó 1986). As it is seen that the population rate of UV Ceti type stars in our Galaxy is about 48.75%, which means that one of each two stars in our

¹Department of Astronomy and Space Sciences, University of Ege, Bornova, 35100 İzmir, Turkey

²Corresponding Author, Email: ali.dal@ege.edu.tr

galaxy shows the flare phenomenon. As it is expected, the general population rate of UV Ceti type stars is incredibly high in both the open clusters and the associations (Mirzoyan 1990; Pigatto 1990). However, the population rate of these stars has a reducing trend, while the age of the cluster gets older due to the Skumanich's law (Skumanich 1972; Pettersen 1991; Stauffer 1991; Marcy & Chen 1992). This is because the mass loss rate is so high due to the flare activity during the main sequence life of the stars that the evolution track of the stars are changed by these mass loss in their main sequence stages, and also in later stages (Marcy & Chen 1992).

According to the recent studies, the mass loss rate of UV Ceti type stars is about $10^{-10} M_{\odot}$ per year due to flare like events, while the solar mass loss rate is about $2 \times 10^{-14} M_{\odot}$ per year (Gershberg 2005). The difference between the mass loss ratios is also seen between the flare energy levels of the solar and stellar cases. As it is generally observed in the case of RS CVn type active binaries (Haisch et al. 1991), the highest energy detected from the most powerful flares, known as two-ribbon flares, occurring on the sun is found to be $10^{30} - 10^{31}$ erg (Gershberg 2005; Benz 2008). On the other hand, the flare energy level varies from 10^{28} erg to 10^{34} erg in the case of dMe stars (Haisch et al. 1991; Gershberg 2005), while some stars of young clusters such as the Pleiades cluster and Orion association exhibit some powerful flare events, which energies reach 10^{36} erg (Gershberg & Shakhovskaya 1983).

Although both the mass loss ratios and the flare energy levels are remarkably different between the solar and stellar cases, the flare events occurring on a dMe star are generally tried to explain by the classical theory of solar flare. The main energy source in the flare events is magnetic reconnection processes in this theory (Gershberg 2005; Hudson & Khan 1997). However, this theory does not figure out each flare phenomenon observed from the UV Ceti type stars. To reach the real solution, examining the flare events occurring on the different type stars, all the differences and similarities should be demonstrated. Then, it should be identified which parameters such as singularity, binarity, mass, age, ect, cause these differences and similarities. For example, some differences are seen between the flare frequencies from one star to the next. The similar case occurs for the flare energy spectra.

In this study, we figured out the nature of a low mass eclipsing binary, KIC 9761199, which is a bit different from the classical UV Ceti type stars from spectral type dMe due to being a binary system. We did complete light curve analyses of the system for the first time in the literature in order to find out the physical properties of the components, using the PHOEBE V.0.32 software (Prša & Zwitter 2005), whose method depends on the 2003 version of Wilson-Devinney Code (Wilson & Devinney 1971; Wilson 1990). Then, the variations out-of-eclipses were analyzed, and the flares occurring on the chromospherically active component were detected to model the magnetic activity nature of the system, comparing the active component with its analogue.

KIC 9761199 (KOI 1459) was listed with the B band brightness of $17^m.2$ in the USNO ACT Catalog (Urban et al. 1997) in the first time literature.

Secondly, KIC 9761199 was listed as J19083435+4630290 in 2MASS All-Sky Survey Catalogue, in which the JHK brightness of the system were given as $J = 13^m.574$, $H = 12^m.926$, $K = 12^m.782$ (Kharchenko 2001; Cutri et al. 2003). Although the orbital period of the system (P_{orb}) was determined as 0.692031 day for the first time by Watson (2006), analyzing the data obtained in the Kepler Mission, Coughlin et al. (2011) indicated that the orbital period of the system (P_{orb}) is 1.3839980 day. There is no any light curve analysis of the system in detail, though Borucki et al. (2011) computed the semi-major axis (a) of the system as $0.013 AB$, while Coughlin et al. (2011) calculated the inclination (i) of the system as $74^\circ.47$ and noted that there is no third light excess. However, they also noted that the system should be examined by a complete light curve analysis in detail.

In the Kepler Database, the $(B - V)$ color index of the system is given as $0^m.068$, while the temperature ratio of the components is given 0.682 by Slawson et al. (2011). In addition, the inclination (i) of the system is listed as $\sin i = 0.99451$. However, this inclination value is not in agreement with $i = 74^\circ.47$ given by Coughlin et al. (2011). According to Walkowicz & Basri (2013), the age of the system is 0.77 Gyr and the $(B - V)$ color index of the system is $1^m.36$.

The one of the spectral studies of the system is belong to Mann et al. (2013) and they gave the luminosity (L) of the system as $0.082 L_\odot$. Using the calibration of some spectral observations, Muirhead et al. (2012) indicated that the system is a binary with components from the spectral type of M1, whose distance is about 198 pc. The total masses given in the literature for the components vary from $0.51 M_\odot$ (Muirhead et al. 2014) to $0.65 M_\odot$ (Coughlin & López-Morales 2012), while the radius vary from $0.48 R_\odot$ (Muirhead et al. 2014) to $0.84 R_\odot$ (Coughlin & López-Morales 2012). The temperature given in the literature for the system varies from 3742 K (Muirhead et al. 2014) to 4060 K (Coughlin & López-Morales 2012). Using the calibrations, Coughlin & López-Morales (2012) calculated mass and radius of each component as $M_1 = 0.646 M_\odot$, $M_2 = 0.444 M_\odot$, $R_1 = 0.830 R_\odot$, $R_2 = 0.384 R_\odot$.

2. DATA AND ANALYSES

The Kepler Mission is one of the space missions to be aimed to find out exo-planet, in which More than 150.000 targets have been already observed (Borucki et al. 2010; Koch et al. 2010; Caldwell et al. 2010). The quality and sensitivity of these observations have the highest one ever reached in the photometry (Jenkins et al. 2010a,b). In these observations, so many variable targets such as new eclipsing binaries, etc. have been also discovered apart from the exo-planets (Slawson et al. 2011; Matijević et al. 2012). There are lots of single or double stars, which some of them are the eclipsing binaries, exhibiting chromospheric activity among these newly discoveries (Balona 2015).

The data analyzed in this study were taken from the Kepler Mission Database (Slawson et al. 2011; Matijević et al. 2012). After removing the

all the observations with large error due to the technical problems from the data, using the ephemeris taken from the Kepler Mission database, the phases were computed for all data used in the analysis, and obtained light curves were shown in Figure 1. Because of this study format, the detrended short cadence data were used in the analysis instead of the long cadence. The data were arranged as the suitable formats to analysis the flare events and also the light curve.

2.1. *Light Curve Analysis*

To compute the flare parameters, it needs the synthetic light curve as assumed the quiescent levels. In this purpose, the light curves shown in the upper panel of Figure 1 were analyzed, after removing the instant-short term light variations due to the flare activity. The initial analyses indicated that there are several solutions according to these data. Because of this, the averages of all the detrended short cadence data were computed phase by phase with interval of 0.001. Then, this averaged light curve shown in Figure 2 was analyzed.

Using the PHOEBE V.0.32 software (Prša & Zwitter 2005), which is employed in the 2003 version of the Wilson-Devinney Code (Wilson & Devinney 1971; Wilson 1990), we analyzed the light curves obtained from the averages of all the detrended short cadence data. We attempted to analyze the light curves in various modes, including the detached system mode (Mod2), semi-detached system with the primary component filling its Roche-Lobe mode (Mod4), and semi-detached system with the secondary component filling its Roche-Lobe mode (Mod5). Our initial analyses demonstrated that an astrophysically reasonable solution was obtainable only in the detached system mode; no results that were statistically consistent with reasonable solutions could be obtained in any of the other modes.

There are several studies about KIC 9761199 in the literature, and lots of temperature values were given for the system varying from 3742 K (Muirhead et al. 2014) to 4060 K (Coughlin & López-Morales 2012). To understand which one is right, in this study, we calculated both $(H - K)$ and $(J - H)$ color indexes from the JHK brightness ($J = 13^m.574$, $H = 12^m.926$, $K = 12^m.782$) given by Kharchenko (2001) and Cutri et al. (2003). Then, using the calibrations determined by Tokunaga (2000), we derived de-reddened colors as $(H - K)_0 = 0^m.15$ and $(J - K)_0 = 0^m.58$. In addition, using the same calibrations, we derived the temperature of the primary component as 4040 ± 20 K depending on these de-reddened colors. In fact, the initial analyses with different temperature values between 3742 K - 4060 K indicated that an astrophysically acceptable solution could be obtained, if the temperature would be taken 4060 K for the primary component. Because of this, in the analysis, the temperature of the primary component was fixed to 4060 K, while the temperature of the secondary component was taken as adjustable parameter. Considering the spectral type corresponding to this temperature, the albedos (A_1 and A_2) and the gravity-darkening coefficients (g_1 and g_2) of the

components were adopted for the stars with the convective envelopes (Lucy 1967; Rucinski 1969). The nonlinear limb-darkening coefficients (x_1 and x_2) of the components were taken from Van Hamme (1993). In the analyses, their dimensionless potentials (Ω_1 and Ω_2), the fractional luminosity (L_1) of the primary component, the inclination (i) of the system, the mass ratio of the system (q), and the semi-major axis (a) were taken as the adjustable free parameters.

The sinusoidal variation out-of-eclipses were modelled with two cool spots on the primary component. In the analysis, although the third light was taken as the adjustable free parameters, it is seen that there is no third light excess in the total light.

All the parameters obtained from the light curve analysis are listed in Table 1. As it can be seen from the table, the error values of each parameter are saliently small. This is caused due to the averaged data used in the analyse. If the original data plotted in the upper panel of Figure 1 were used in the analyse, it would be waiting that the error values are more larger. In addition, apart from some theoretical parameters such as the nonlinear limb-darkening coefficients (x_1 and x_2), the albedos (A_1 and A_2) and the gravity-darkening coefficients (g_1 and g_2), the temperature of the primary component is just one parameter to fixed in the analysis. However, the temperature of the primary component was not also arbitrary determined. This temperature was determined from the JHK data of system given in the 2MASS All-Sky Survey Catalogue. As a result, the parameters found from the light curve analysis in Table 1 are absolutely trustworthy to figure out the obvious nature of KIC 9761199.

The synthetic light curve obtained with these parameters is shown in Figure 2. In this figure, both primary and secondary minima of the light curve are also plotted in the wide plane to better view for the readers. In addition, the 3D model of Roche geometry depending on these parameters is shown in Figure 3. The Roche geometry and the cool spot locates depending on the parameters obtained from the light curve analysis is shown for different phases, such as the phases of 0.00, 0.25, 0.50, 0.75.

Although there is not any available radial velocity curve, we tried to estimate the absolute parameters of the components. Considering the calibrations given by Tokunaga (2000), $(B - V)$ color index was found to be $1^m.303$ for the primary component depending on its temperature value derived from the analysis, while it was found to be $1^m.378$ for the secondary components. These color indexes are in agreement with the value found by Walkowicz & Basri (2013). Using the calibrations given by Tokunaga (2000), the mass of the primary component must be $0.57 \pm 0.01 M_\odot$ corresponding to its $(B - V)$ color index. Considering the possible mass ratio of the system, the mass of the secondary component was found to be $0.39 \pm 0.02 M_\odot$. Using Kepler's third law, we calculated the possible semi-major axis as a $5.16 \pm 0.02 R_\odot$. Considering this estimated semi-major axis, the radius of the primary component was computed as $0.62 \pm 0.05 R_\odot$, while that of the secondary component was

computed as $0.56 \pm 0.05 R_{\odot}$.

2.2. Flare Activity and the OPEA Model

To demonstrate the chromospherically active nature of the system, it needs to reveal the light variations just due to flare events. For this aim, first of all, all the light variations due to both the geometrical effects and the rotational modulation caused by the spots were removed from the general light variation. For this purpose, the data of all the pre-whitened light curves were obtained. To acquire the pre-whitened data, we extracted the synthetic light curves from all the detrended short cadence data.

In the second step, to determine the basic flare parameters such as the first point of the flare beginning, the last point of the flare end and the flare energy, the quiescent levels for each flare should be derived. In this point, the synthetic model lead us to definite the quiescent levels for each flare at the same time of that flare. Using the synthetic model as the quiescent levels, the parameters of the flares were computed. Two samples of the flare light curves taken from observation data and the quiescent levels derived for these flares are shown in Figures 4.

Using the synthetic models assumed as the quiescent levels, both the beginning and the end of a flare for each one were defined, and then, some flare parameters, such as flare rise times (T_r), decay times (T_d), amplitudes of flare maxima, flare equivalent durations (P), were computed. In total, 94 flare were detected from the available short cadence data in the Kepler Mission Database. All the computed parameters are listed in Table 2 for these 94 flares. In the table, flare maximum times, equivalent durations, rise times, decay times and amplitudes of flare maxima are listed from the first column to the last, respectively.

In the analysis, the equivalent durations of the flares were computed using Equation (1) taken from Gershberg et al. (1972):

$$P = \int [(I_{flare} - I_0)/I_0] dt \quad (1)$$

where I_0 is the flux of the star in the observing band while in the quiet state. In this study, we computed I_0 using by the synthetic models derived with the light curve analysis. I_{flare} is the intensity observed at the moment of the flare. P is the flare-equivalent duration in the observing band. In this study, the flare energies (E) were not computed to be used in the following analyses due to the reasons described in detail by Dal & Evren (2010, 2011).

Examining the relationships of the flare parameters among each other, it is seen that the distributions of flare equivalent durations on the logarithmic scale versus flare total durations are varying according to a rule. The distributions of flare equivalent durations on the logarithmic scale cannot be higher than a specific value for the star, and it is no matter how long the

flare total duration is. Using the SPSS V17.0 (Green et al. 1999) and GraphPad Prism V5.02 (Dawson & Trapp 2004) programs, Dal & Evren (2010, 2011) indicated that the best function is the One Phase Exponential Association (hereafter OPEA) for the distributions of flare equivalent durations on the logarithmic scale versus flare total durations. The OPEA function has a *Plateau* term, and this makes it a special function in the analyses. The OPEA function is defined by Equation (2):

$$y = y_0 + (Plateau - y_0) \times (1 - e^{-k \times x}) \quad (2)$$

where the parameter y is the flare equivalent duration on a logarithmic scale, the parameter x is the flare total duration, according to the definition of Dal & Evren (2010), and the parameter y_0 is the flare-equivalent duration in on a logarithmic scale for the least total duration. In other words, the parameter y_0 is the least equivalent duration occurring in a flare for a star. Here is an important point that the parameter y_0 does not depends on only flare mechanism occurring on the star, but also depends on the sensitivity of the optical system used for the observations. The parameter *Plateau* value is upper limit for the flare equivalent duration on a logarithmic scale. Dal & Evren (2011) defined *Plateau* value as a saturation level for a star in the observing band.

Using the least-squares method, the OPEA model was derived for the distributions of flare equivalent durations on the logarithmic scale versus flare total durations. The derived model is shown in Figure 5 together with the observed flare equivalent durations, while the parameters computed from the model are listed in Table 3. The *span* value listed in the table is difference between *Plateau* and y_0 values. According to the definition of the OPEA function, the parameter k in Equation (2) is a constant for just this model, depending on the x values. The *half-life* value is half of the first x value, at which the model reaches the *Plateau* value. In other words, it is half of the minimum flare total time, which is enough to the maximum flare energy occurring in the flare mechanism.

It was tested by using three different methods, such as the D'Agostino-Pearson normality test, the Shapiro-Wilk normality test and also the Kolmogorov-Smirnov test, given by D'Agostino & Stephens (1986) to understand whether there are any other functions to model the distributions of flare equivalent durations on the logarithmic scale versus flare total durations. In these tests, the probability value called as *p-value* was found to be *p-value* < 0.001 and this means that there is no other function to model the distributions of flare equivalent durations (Motulsky 2007; Spanier & Oldham 1987).

KIC 9761199 was observed as long as 289.82931 day from JD 2455641.50631 to JD 2455931.33562 without any remarkable interruptions. In total, significant 94 flares were detected in these observations. The total flare equivalent duration computed from all the flares was found to be 628.11671 s (0.17448 hours). Ishida et al. (1991) described two frequencies for the stellar flare activity. These frequencies are defined as given by Equations (3) and (4):

$$N_1 = \Sigma n_f / \Sigma T_t \quad (3)$$

$$N_2 = \Sigma P / \Sigma T_t \quad (4)$$

where Σn_f is the total flare number detected in the observations, and ΣT_t is the total observing duration, while ΣP is the total equivalent duration obtained from all the flares. In this study, N_1 frequency was found to be 0.01351 h^{-1} , while N_2 frequency was found to be 0.00006.

3. RESULTS AND DISCUSSION

The results obtained from the analyses of short cadence data in the Kepler Mission Database indicated that KIC 9761199 exhibits high level chromospheric activity. However, it needs to identify which component is active, then, it should be compared with its analogue to be certain about activity level of the system. All these need to determine the physical parameters of the components, firstly.

Although all the variations apart from the geometrical effect, such as flare activity, were removed from the short cadence data taken from the database, neither the eclipses nor any other variation could be seen clearly in these eliminated data, as it is seen from the upper panel of Figure 1. To use in the light curve analysis, we computed the averages phase by phase with interval of 0.001 for the eliminated short cadence data. As it can be seen from Figure 2, both the primary and secondary minima and also a sinusoidal variation due to the rotational modulation are clearly visible in these averaged data. Here is an important point that the amplitude difference between the primary and secondary minima can be visible. This is important, because the orbital period of the system is a controversial point in the literature (Watson 2006; Coughlin et al. 2011). However, this figure demonstrates that the orbital period of the system is 1.3839980 day, not 0.692031 day. According to this result, first of all, KIC 9761199 is a double object. There are two different minima, because of this, the secondary object can not be a planet, it must be a star. If it was a planet, there would not be any secondary minimum in the light curve due to the contrast effect between a star and a planet.

In the literature, although there are a few approaches using some calibrations for the physical parameters of the components, there is no complete light curve analysis for KIC 9761199. In this purpose, the light curve obtained from the detrended short cadence data was analyzed, using the PHOEBE V.0.32 software (Prša & Zwitter 2005), which is employed in the 2003 version of the Wilson-Devinney Code (Wilson & Devinney 1971; Wilson 1990). Although the spectral type was given as M1V for KIC 9761199 (Muirhead et al. 2012), there are several temperature values mentioned for this system. According to the de-reddened colors $(H - K)_0 = 0^m.15$ and $(J - K)_0 = 0^m.58$ of

the system, the temperature of the primary component was taken 4060 K as given by Coughlin & López-Morales (2012). In the light curve analysis with the PHOEBE V.0.32 software, the temperature of the secondary component was found to be 3891 ± 1 K. The mass ratio of the system (q) was found to be 0.69 ± 0.01 , while the inclination (i) of the system was found to be $77^\circ.44 \pm 0^\circ.01$.

In addition, as it is seen from Figure 1 and the upper panel of Figure 2, the light curve exhibits a remarkable sinusoidal variation at out-of-eclipses. This variation could be caused by the effects of tidal distortion or the mutual heating of the components themselves. All these cases were included to the analysis. For this aim, the albedos (A_1 and A_2), the gravity-darkening coefficients (g_1 and g_2) of the components were computed depending on their temperatures and their dimensionless potentials (Ω_1 and Ω_2) were also derived in the analysis. However, it was seen from the initial results that the synthetic light curve obtained with these parameters did not fit the observations. In this point, considering both the temperatures and the fractional radii of the components, and also considering the flare activity, we assumed that this sinusoidal variation is caused by the rotational modulation due to the stellar cool spots. Because of this, the sinusoidal variation was modelled with two cool spots on the primary component in the light curve analysis. The spots are separated by about 180° longitudinally, while one of them is located about the latitudes of $47^\circ.0 \pm 0^\circ.2$ and the other one is located about the latitudes of $30^\circ.0 \pm 0^\circ.2$. Here, it must be noted that it was assumed the cool spots locate on the primary component. However, it is likely they can be located on the secondary component, too. Someone can easily reach an acceptable solution, astrophysically. A strong clue for the answer of this quandary is come from the discussion of flare activity in the later part of the text. The 3D model of Roche geometry for the components and also the cool spots on the primary component is shown in Figure 3 for different phases.

Considering both the component temperatures and fractional radii found from the light curve analysis, using the calibrations given by Tokunaga (2000), and also Kepler's third law, we tried to estimate the absolute parameters of the components. The mass of the primary component found be $0.57 \pm 0.01 M_\odot$ while it was found to be $0.39 \pm 0.02 M_\odot$ for the secondary component. In addition, the radius of the primary component was computed as $0.62 \pm 0.05 R_\odot$, while that of the secondary component was computed as $0.56 \pm 0.05 R_\odot$.

When it is considered the results of the analysis, it is seen that both the locations of the stellar spots are not changed on the primary component along 289.82931 day (9.66 months), during all the observing season. However, this is a serious moot point for the astrophysical perspective, because a spotted area evolves in 2 or 3 months at most in the solar case (Gershberg 2005). On the other hand, according to Hall et al. (1989) and Gershberg (2005), it is well known that the spotted areas on the active components of some RS CVn binaries, such as V478 Lyr, can keep their shapes and locations about two years. Therefore, the behaviour of the cool spot activity observed in the

case of KIC 9761199 is not inconsistent event in respect to the stellar spot activity phenomenon. It must be noted that although we stated the word spot, actually it refers to an active area, in which several spots can appear and disappear in time. Here, the question to be answered is why the locations of these areas are stable for 289.82931 days. This is a discussion about the differential rotation of the components.

We detected 94 flare events from KIC 9761199, and calculated some parameters for each flare, such as flare frequencies. Yoldaş & Dal (2016) recently resolved the chromospheric activity nature of a different system, FL Lyr. They found both flare frequencies as $N_1 = 0.41632 \text{ h}^{-1}$ and $N_2 = 0.00027$ for that system. Comparing the flare frequencies of KIC 9761199 with those of FL Lyr, it is clearly seen that FL Lyr exhibits flare more frequently than KIC 9761199, and also its flares are more powerful than those of KIC 9761199. Comparing KIC 9761199's flare frequency values with those found for UV Ceti type flare stars from spectral type dK5e to dM6e, the flare energies obtained from KIC 9761199 are remarkably lower than those obtained from UV Ceti stars. For instance, the observed flare number per hour for AD Leo was found to be $N_1 = 1.331 \text{ h}^{-1}$, while it was found to be $N_1 = 1.056 \text{ h}^{-1}$ for EV Lac. Moreover, N_2 frequency was found to be 0.088 for EQ Peg, while it was found to be $N_2 = 0.086$ for AD Leo (Dal & Evren 2011). As it is clearly seen from these results, the flare frequencies of KIC 9761199 are remarkably small. However, it is well known from Dal & Evren (2011) that the flare frequency can dramatically changes from one season to the next for some stars, such as V1005 Ori, EV Lac, etc. In this case, there could be some changes in the flare frequency and the flare behaviour of KIC 9761199 in the next observing seasons. In addition, these results found from the flare frequency analyses reveal why any flare had not been detected from this system by any ground based telescope before the Kepler Mission. If N_2 frequency is especially considering, it will be understandable, because, N_2 frequency indicates that the flare events occurring on the active component of the system are so weak to observe by any ground based telescope.

The *Plateau* value was found to be $1.951 \pm 0.069 \text{ s}$ from the OPEA model derived from the variation of the flare equivalent duration distributions on the logarithmic scale versus flare total durations for 94 flares. However, Yoldaş & Dal (2016) found the *Plateau* value as $1.232 \pm 0.069 \text{ s}$ for FL Lyr. Moreover, Dal & Evren (2011) computed the *Plateau* values for some UV Ceti type stars. They gave the *Plateau* values as 3.014 s for EV Lac ($B - V = 1^m.554$) and 2.935 s for EQ Peg ($B - V = 1^m.574$), and also it is 2.637 s for V1005 Ori ($B - V = 1^m.307$). As it is seen that the maximum flare energy detected from KIC 9761199 is remarkably smaller than the maximum energy level obtained from UV Ceti type single flare stars. The *Plateau* value of this system a bit approaches just to the value obtained from V1005 Ori. It must be noted that Dal & Evren (2011) found that the *Plateau* value is always constant for a star, while it is changing from one star to the other depending on their $B - V$ color indexes. The authors defined the *Plateau* value as the

energy saturation level for the flare mechanism occurring on the star. As a result, the flare activity should be occurred on the primary component due to its $B - V$ color index. If it would be the secondary component, the *Plateau* value of KIC 9761199 was seen a bit incompatible according to the analogue of the secondary component.

Using the regression calculations, the *half - life* value was found to be 1014.0 s from the OPEA model for KIC 9761199. In the case of FL Lyr, it is 2291.7 s (Yoldaş & Dal 2016). It means that a flare occurring on the FL Lyr can reach the maximum energy level when the flare total duration reaches $n \times 38$ minutes, while it takes $n \times 17$ minutes for KIC 9761199. Here n is a constant depending on the OPEA function of a star (Spanier & Oldham 1987; Dawson & Trapp 2004; Motulsky 2007). In other words, the parameter *half - life* refers a minimum duration limit for a flare reached maximum energy. In this perspective, the flares, whose total times are shorter than $n \times 17$ minutes, can never reach the *Plateau* value obtained from the OPEA model derived for the flares of KIC 9761199. This value is a few times higher than those obtained from single dMe stars. Because, in the case of single dMe stars, for example, it was found to be 433.10 s for DO Cep ($B - V = 1^m.604$), and 334.30 s for EQ Peg, while it is 226.30 s for V1005 Ori (Dal & Evren 2011). It means that in the case of the stars such as EQ Peg, V1005 Ori and DO Cep, the flares can reach the maximum energy level at their *Plateau* value, when their total durations reach about $n \times 5$ minutes, while it needs $n \times 17$ minutes for KIC 9761199.

On the other hand, maximum flare rise time (T_r) obtained from the flares of eclipsing binary KIC 9761199 was found to be 1118.098 s, while maximum flare total time (T_t) was found to be 6767.72 s. However, these values are $T_r = 5179.00$ s and $T_t = 12770.62$ s for FL Lyr. As a result, FL Lyr flare time scales are larger than those obtained from KIC 9761199, which is in agreement with the results found by Dal & Evren (2011) for the single flare stars from dMe. In the light curve analysis, the primary component is assumed as the chromospherically active component and its color index was found to be $(B - V) = 1^m.303$. However, the $(B - V)$ color index of the active component of FL Lyr is $0^m.74$. Consequently, the chromospherically active component of KIC 9761199 is cooler than that of FL Lyr. In this case, the flare time scales of FL Lyr must be larger than the other according to Dal & Evren (2011).

Finally considering the *Plateau* value, flare frequencies and also flare time scales, it is clearly seen that the flare activity level of KIC 9761199 is clearly lower than almost all the UV Ceti type stars, as it is in the case of FL Lyr. This result about the chromospheric activity level of the system is also in agreement with the result found by Dal & Evren (2011). The author indicated that all these parameters derived from the OPEA model of a star are depend on just the $(B - V)$ color index of that star. In other word, the OPEA model parameters increase or decrease according to variation of the $(B - V)$ color index from a star to the other. As a matter of course, the OPEA model parameters derived for KIC 9761199 were found as expected values for the

$(B - V)$ color index of the primary component, not the secondary component.

In this point, it could be better to recapitulate that comparing the flare activity nature seen from KIC 9761199 indicated that the assumption of "the chromospherically active star is the primary component of the system" is correct. In addition, the statistical analyses of the OPEA model demonstrated that there is only one star exhibiting the flare activity in the system. Because, according to the statistical analyses, the probability value found to be $p - value < 0.001$. It means that there is no other function to model the distributions of flare equivalent durations (Motulsky 2007; Spanier & Oldham 1987). Therefore, there is only one star exhibiting flare activity, in front of us. Considering the classical theory of solar flare (Gershberg 2005), the star exhibiting flare activity and cool spot activity must be the same star.

According to Dal & Evren (2011), it is a contentious issue which parameter, the *Plateau* value or the flare frequencies (N_i), is the best indicator for the activity level. In general, the chromospheric activity level of a system depends on some parameters such as especially stellar rotation velocity. The rotation velocity depends on generally the stellar age or being a component of a close binary. Because of this, we discussed KIC 9761199 for both cases. Firstly, the age of KIC 9761199 is given as 0.77 Gyr (Walkowicz & Basri 2013), while the age of FL Lyr is given between 3.05 Gyr and 15.25 Gyr in the literature. Considering Skumanich (1972)'s law, it would be expected that the activity level of KIC 9761199 is clearly higher than that of FL Lyr. Secondly, in this study we computed the radii of the components as $R_1 = 0.62 R_\odot$ and $R_2 = 0.56 R_\odot$, and the semi-major axis as $5.16 R_\odot$. However, the radii of the FL Lyr components are given as $R_1 = 1.283 R_\odot$, $R_2 = 0.963 R_\odot$, and its semi-major axis is given as $a = 9.17 R_\odot$ by Eker et al. (2014). According to these absolute parameters of the systems, the activity level of KIC 9761199 should be higher than FL Lyr activity level. If the flare frequencies (N_i) are considered, the flare frequencies of FL Lyr are higher than KIC 9761199. However, if the *Plateau* values are considered, the *Plateau* value of KIC 9761199 is clearly higher than that of FL Lyr. According to the semi-major axis of the KIC 9761199, the components are closer to the each other than the status of FL Lyr's components. Maybe this is why the *Plateau* value is higher in the case of KIC 9761199. However, there is still an unsolved point yet. Why the flare frequencies are higher in the case of FL Lyr? The similar phenomenon is also common among the UV Ceti type single stars (Dal & Evren 2010, 2011).

As a result, according to possible masses and radii of the components, KIC 9761199 must be a low-mass and a close binary system. In addition, according to the OPEA model parameters, just one component of the system is chromospherically active star. Both the age given in the literature and the proximity of the components can help to keep the activity level as possible as high. However, the active component exhibits intense flare activity, while it exhibits quiescent spot activity. It does not mean that the cool spot activity level is low in this system. It is possible that the active component could be covered by some large spots spread to the all surface. In this case, there

would be no rapid light variation in the light curve out-of-eclipses contrary to the case of FL Lyr. To reveal and understand the nature of the cool spot activity in this system, it needs to track the sinusoidal light variation due to the rotational modulation in the light curve. However, these observations will be very difficult for the ground based telescope due to the sensitivity problems. In addition, there is no detailed spectroscopic observation of the KIC 9761199 in the literature. Therefore, it is also needed for the future studies.

Acknowledgments

The authors thank the referee for useful comments that have contributed to the improvement of the paper.

REFERENCES

- Balona, L.A., 2015, MNRAS, 447, 2714
- Benz, A.O., 2008, Living Rev. Solar Phys., 5, 1
- Borucki, W.J., Koch, D.G., Basri, G., et al., 2010, Sci, 327, 977
- Borucki, W.J., Koch, D.G., Basri, G., et al., 2011, ApJ, 736, 19
- Caldwell, D.A., Kolodziejczak, J.J., & Van Cleve, J. E., 2010, ApJL, 713, L92
- Coughlin, J.L., López-Morales, M., Harrison, T.E., et al., 2011, AJ, 141, 78
- Coughlin, J.L., López-Morales, M., 2012, AJ, 143, 39
- Cutri, R.M., Skrutskie, M.F., van Dyk, S., et al., 2003. The IRSA 2MASS all sky point source catalog. NASA IPAC Infrared Science Archive <http://irsa.ipac.caltech.edu/applications/Gator>
- D'Agostino, R. B. & Stephens, M.A., 1986, "Tests for Normal Distribution" in Goodness-Of-Fit Techniques, Statistics: Textbooks and Monographs, New York: Dekker, edited by D'Agostino, R.B., Stephens, M.A.
- Dal, H.A. & Evren, S., 2010, AJ, 140, 483
- Dal, H.A. & Evren, S., 2011, AJ, 141, 33
- Dal, H.A., Sipahi, E., Özdarcan, O., 2012, PASA, 29, 150
- Dawson, B. & Trapp, R.G., 2004, "Basic and Clinical Biostatistics" (New York: McGraw-Hill), 61
- Eker, Z., Bilir, S., Soyduğan, F., et al., 2014, PASA, 31, 24
- Gershberg, R. E. & Shakhovskaya, N. I., 1983, Astrophys. Space Sci., 95, 235
- Gershberg, R.E., 1972, Astrophys. Space Sci., 19, 75
- Gershberg, R.E., 2005, "Solar-Type Activity in Main-Sequence Stars", Springer Berlin Heidelberg, New York, p.53, 191, 360
- Green, S.B., Salkind, N.J. & Akey, T.M., 1999, "Using SPSS for Windows: Analyzing and Understanding Data" (Upper Saddle River, NJ: Prentice Hall), 50
- Haisch, B., Strong, K.T., Rodonó, M., 1991, ARA&A, 29, 275
- Hall D.S., Henry G.W., Sowell J.R., 1989. AJ, 99, 396.
- Hudson, H.S. & Khan, J.I., 1997, in ASP Conf. Ser. 111, "Magnetic Reconnection in the Solar Atmosphere", ed. R. D. Bentley & J. T. Mariska (San Francisco, CA: ASP), 135
- Ishida, K., Ichimura, K., Shimizu, Y., et al., 1991, Ap&SS, 182, 227
- Jenkins, J.M., Caldwell, D.A., Chandrasekaran, H., et al., 2010a, ApJL, 713, L87
- Jenkins, J.M., Chandrasekaran, H., McCauliff, S.D., et al., 2010b, Proc. SPIE, 7740, 77400
- Kharchenko, N.V., 2001, KFNT, 17, 409
- Koch, D.G., Borucki, W.J., Basri, G., et al. 2010, ApJL, 713, L79
- Lucy, L.B., 1967, Z. Astrophys, 65, 89
- Mann, A.W., Gaidos, E., Ansdell, M., 2013, ApJ, 779, 188
- Marcy, G.W. & Chen, G.H., 1992, ApJ, 390, 550
- Matijević, G., Prša, A., Orosz, J.A., et al. 2012, AJ, 143, 123
- Mirzoyan, L.V., 1990, in IAU Symp. 137, "Flare stars in star clusters, associations and the solar vicinity", proceedings of the 137th IAU Symposium, Byurakan, Armenian SSR, Oct. 23-27, 1989 (A91-55760 24-90). Dordrecht, Netherlands, Kluwer Academic Publishers, 1990, p.1
- Motulsky, H., 2007, "GraphPad Prism 5: Statistics Guide", San Diego, CA: Graph-Pad Software Inc. Press, 94
- Muirhead, P.S., Becker, J., Feiden, G.A., et al., 2014, ApJS, 213, 5
- Muirhead, P.S., Hamren, K., Schlawin, E., et al., 2012, ApJL, 750, 37

- Pettersen, B.R., 1991, *Mem. Soc. Astron. Ital.*, 62, 217
- Pigatto, L., 1990, in *IAU Symp. 137*, "Flare stars in star clusters, associations and the solar vicinity", proceedings of the 137th IAU Symposium, Byurakan, Armenian SSR, Oct. 23-27, 1989 (A91-55760 24-90). Dordrecht, Netherlands, Kluwer Academic Publishers, 1990, p.117
- Prša, A. & Zwitter, T., 2005, *ApJ*, 628, 426
- Rodonó, M., 1986, *NASSP*, 492, 409
- Rucinski, S.M., 1969, *AcA*, 19, 245
- Skumanich, A., 1972, *ApJ* 171, 565.
- Slawson, R., Prša, A., Welsh, W.F., et al. 2011, *AJ*, 142, 160
- Spanier, J. & Oldham, K.B., 1987, "An Atlas of Function", Washington, DC: Hemisphere Publishing Corporation Press, 233
- Stauffer, J.R., 1991, in *Proc. "NATO Advanced Research Workshop on Angular Momentum Evolution of Young Stars"*, ed. S. Catalano & J.R. Stauffer (Dordrecht: Kluwer), 117
- Tokunaga, A.T. 2000, in *Allen's Astrophysical Quantities*, ed. A.N. Cox (Springer), p.143
- Urban, S., Corbin, T., Wycoff, G., 1997, *AAS*, 191, 5707
- Van Hamme, W., 1993, *AJ*, 106, 2096
- Walkowicz, L.M. & Basri, G.S., 2013, *MNRAS*, 436, 1883
- Watson, C.L., 2006, *SASS*, 25, 47
- Wilson, R.E., 1990, *ApJ*, 356, 613
- Wilson, R.E., Devinney, E.J., 1971, *ApJ*, 166, 605
- Yoldaş, E. and Dal, H.A., 2016, *PASA*, 33, 16

Department of Astronomy and Space Sciences, University of Ege,
Bornova, 35100 İzmir, Turkey (HAD, ali.dal@ege.edu.tr, EY, ezgiy-
oldas@gmail.com).

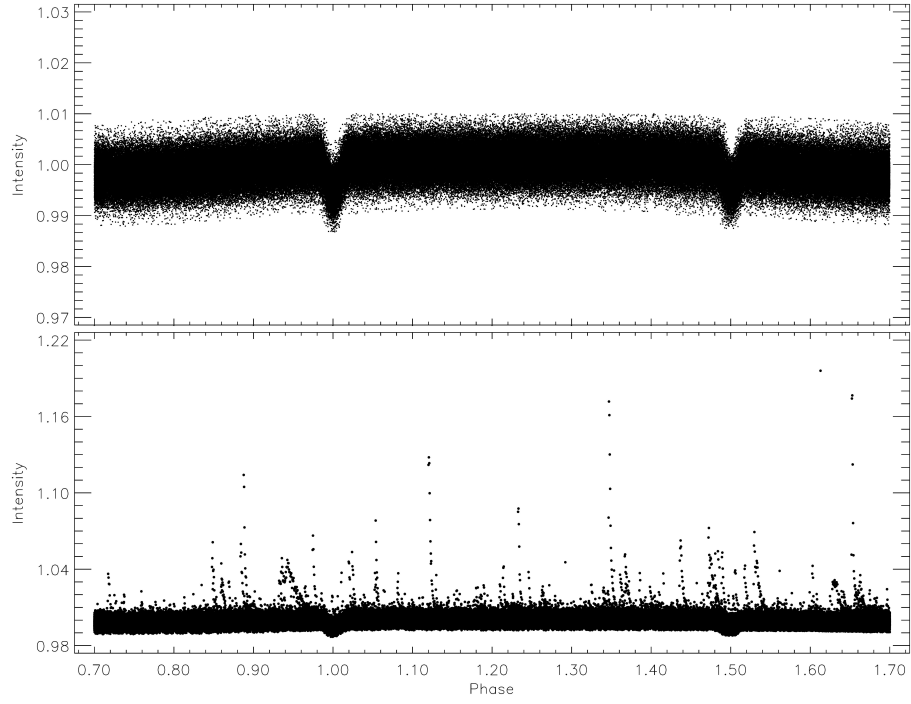


Fig. 1. All the light curve of KIC 9761199 obtained from the detrended short cadence data taken from the Kepler Mission database. In the bottom panel, the light curve was plotted with the flare activity, while the light curve was plotted without the flare activity in the upper panel.

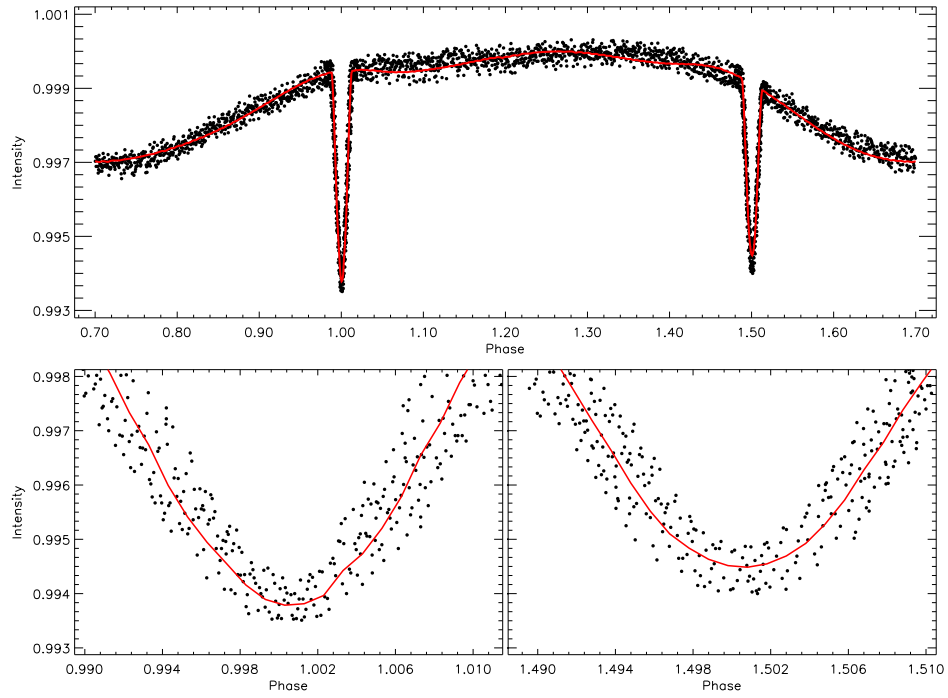


Fig. 2. The observed (filled circles) and synthetic (red smooth line) light curves obtained from the averaged short cadence data acquired from HJD 24 54964.50251 to 24 56424.01145. In the bottom panels of the figure, the minima are plotted in the wide plane to better view.

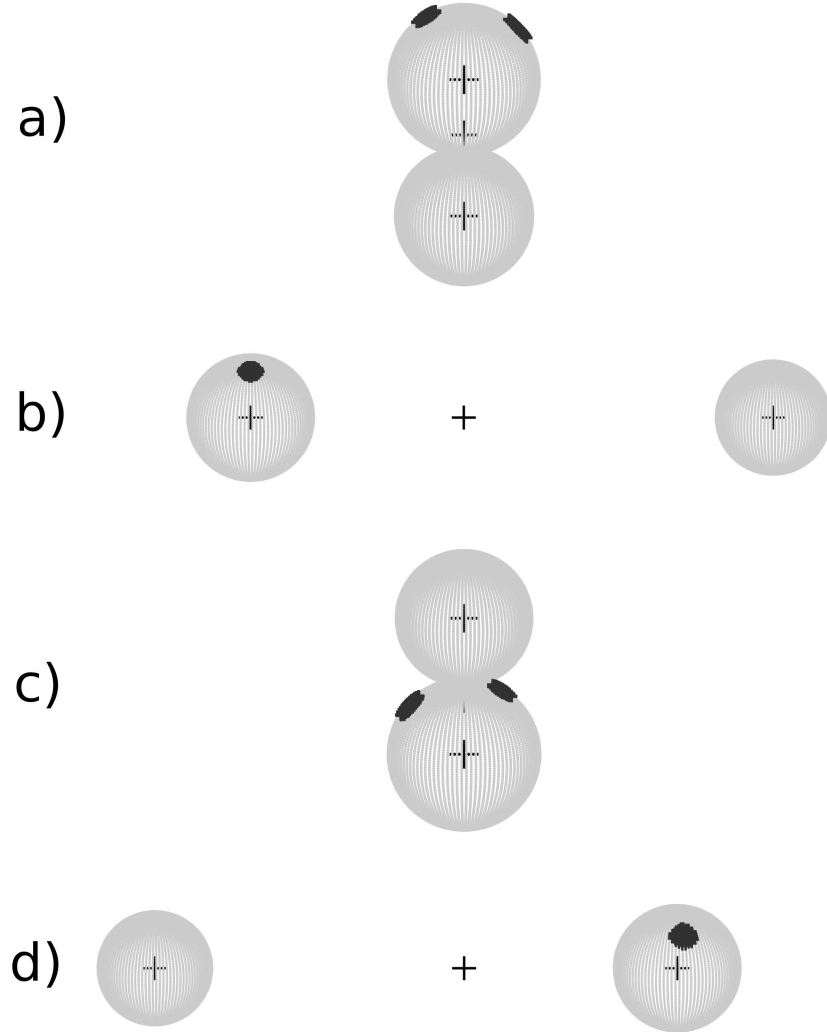


Fig. 3. The 3D model of Roche geometry and the cool spots depending on the parameters obtained from the light curve analysis is shown for different phases, such as a) 0.00, b) 0.25, c) 0.50, d) 0.75.

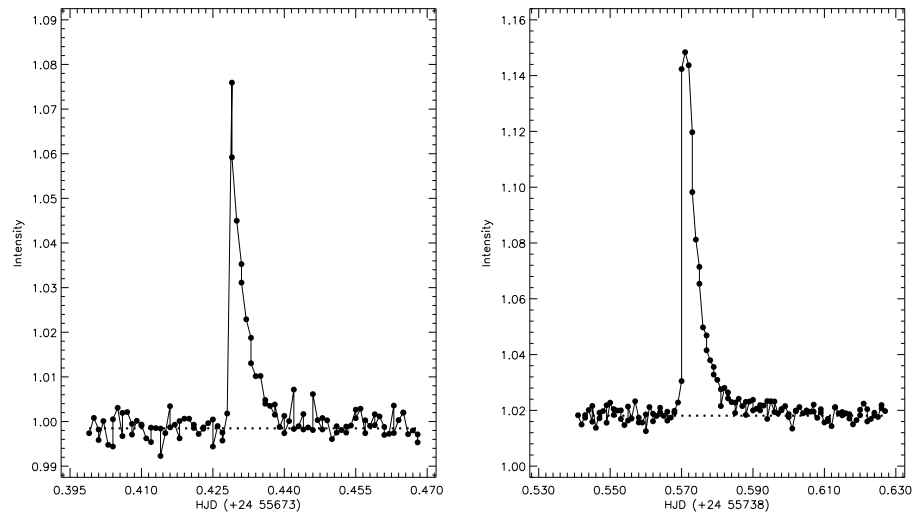


Fig. 4. Two different samples for the flare light variations. In the figure, the filled circles represent the observations, while the dotted lines represent the synthetic light curve obtained by the light curve analysis, which was assumed as the quiescent levels for each flare.

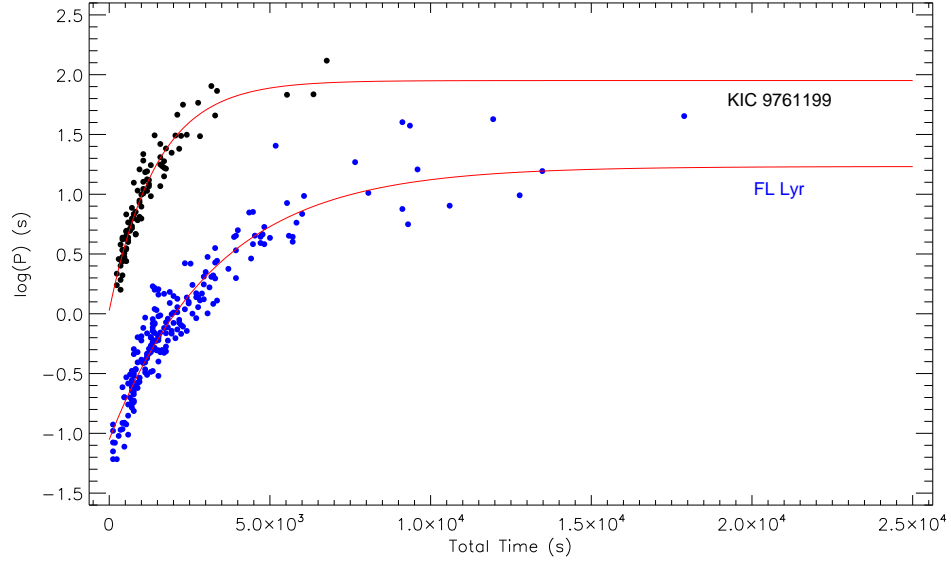


Fig. 5. The OPEA model derived from 94 flares detected in the available short cadence data of KIC 9761199 in the Kepler Mission Database is shown, comparing to the OPEA model obtained from the data of well known eclipsing binary, FL Lyr (Yoldaş & Dal 2016). In the figure, the filled circles represent the calculated $\log(P)$ values from observation, while the lines represent the OPEA models.

TABLE 1

THE PARAMETERS OBTAINED FROM THE LIGHT CURVE ANALYSIS OF KIC 9761199.

Parameter	Value
q	0.69 ± 0.01
$i(^{\circ})$	77.4 ± 0.1
$T_1(K)$	4060 (fixed)
$T_2(K)$	3891 ± 1
Ω_1	8.96 ± 0.03
Ω_2	7.47 ± 0.03
L_1/L_T	0.61 ± 0.02
g_1, g_2	0.32 (fixed)
A_1, A_2	0.50 (fixed)
$x_{1,bol}, x_{2,bol}$	0.696, 0.686 (fixed)
x_1, x_2	0.709, 0.700 (fixed)
$\langle r_1 \rangle$	0.121 ± 0.001
$\langle r_2 \rangle$	0.109 ± 0.001
$Co - Lat_{SpotI} (rad)$	0.82 ± 0.03
$Long_{SpotI} (rad)$	1.71 ± 0.03
$R_{SpotI} (rad)$	0.18 ± 0.01
T_{fSpotI}	0.94 ± 0.01
$Co - Lat_{SpotII} (rad)$	0.52 ± 0.03
$Long_{SpotII} (rad)$	4.71 ± 0.03
$R_{SpotII} (rad)$	0.16 ± 0.01
$T_{fSpotII}$	0.95 ± 0.01

TABLE 2

THE FLARE PARAMETERS COMPUTED FROM KIC 9761199'S THE AVAILABLE SHORT
CADENCE DATA IN THE KEPLER MISSION DATABASE.

Flare Time (+24 00000)	P (s)	T_r (s)	T_d (s)	Amplitude (Intensity)
55648.62149	10.66427	294.25248	882.75744	0.03506
55654.62302	3.46467	117.70704	411.95088	0.01650
55656.57790	2.75499	58.84877	470.80915	0.01424
55657.21749	4.84865	117.69840	411.95952	0.02263
55668.99378	6.77842	117.69840	411.95261	0.03122
55671.88592	5.40725	235.39594	470.81088	0.02135
55673.42871	21.66523	58.85741	1000.46189	0.07746
55682.84894	23.99511	353.10384	1824.38525	0.02916
55690.01663	7.87550	176.55667	823.90608	0.02173
55690.40829	3.41761	176.55667	235.39680	0.01292
55691.66023	2.52343	176.54717	176.55667	0.01662
55691.88910	2.80804	58.75200	294.62400	0.01503
55693.20098	8.51286	235.41408	706.20768	0.02361
55694.47881	13.31688	353.10384	823.92336	0.02229
55694.63820	2.09756	176.55581	235.40544	0.01227
55696.43438	6.47066	353.11248	588.51706	0.01321
55697.18023	15.54061	353.10384	823.90522	0.04237
55698.16517	4.10949	117.69840	470.81002	0.01660
55701.69145	30.56748	411.96125	2412.88330	0.03340
55710.67574	11.65687	176.53853	1059.31757	0.02503
55710.97272	4.24631	176.55581	294.25421	0.02309
55716.28700	18.88827	294.25334	1412.41018	0.04641
55719.31808	10.14314	176.55494	882.76003	0.02788
55722.99896	11.08245	235.39507	823.91818	0.03130
55724.14396	9.62495	176.54630	1118.16202	0.02696
55724.95043	4.94587	117.68890	411.96816	0.01795
55728.06529	56.09567	235.39507	2059.76563	0.07023
55730.64953	13.13169	176.54544	1059.31066	0.02468
55731.55544	2.16425	117.68890	117.70618	0.01401
55733.11593	3.79166	117.69754	235.40285	0.02496
55733.13705	1.92040	235.39421	117.70618	0.01899
55733.40201	12.70762	117.69754	941.60362	0.03861
55738.40292	12.15108	176.55408	1059.30720	0.02349
55738.57116	58.17733	294.25939	2471.71478	0.13029
55740.56212	11.68516	176.54544	1412.40586	0.02275
55744.06656	2.99633	235.40198	235.40198	0.01388
55744.08495	1.73474	117.68803	117.70531	0.01503
55754.92383	130.99219	647.35459	6120.36691	0.04921
55772.29873	19.12241	235.40717	823.88189	0.05312
55773.26593	1.58905	58.84704	294.25421	0.01069
55774.78756	2.74595	176.55062	235.38989	0.01329
55775.25413	6.79622	58.85568	706.17744	0.02373
55775.61308	30.78613	176.55062	2059.71811	0.06187
55783.59719	80.32655	235.38816	2942.44013	0.17808
55785.26730	12.48313	117.69408	647.34250	0.04444
55785.57517	16.66883	176.54112	1530.07402	0.03594
55787.04434	2.90663	235.38816	235.40458	0.01604
55788.38615	5.19716	117.69322	588.49546	0.01873
55788.73897	17.18207	176.53162	1471.22438	0.03291

TABLE 2

CONTINUED FROM PREVIOUS PAGE.

Flare Time (+24 00000)	P (s)	T_r (s)	T_d (s)	Amplitude (Intensity)
55791.99062	15.28898	117.69408	1000.42128	0.03837
55795.39620	2.86915	117.70186	176.54890	0.01564
55819.27527	45.55776	706.16794	2589.28704	0.06316
55796.34364	3.53016	58.85482	470.78237	0.01915
55801.73670	5.81090	176.54803	411.93360	0.02571
55804.52926	2.98768	117.70099	294.24038	0.01691
55820.37526	14.11267	353.08310	1353.48883	0.01976
55805.77229	68.48297	235.38557	6120.19670	0.02991
55806.37235	4.65150	235.38557	588.47990	0.01775
55809.49865	46.23526	882.71856	1235.79562	0.05201
55810.42632	4.35491	235.38470	353.08570	0.01401
55813.21546	17.71834	176.53853	1412.35747	0.03683
55814.02734	4.33411	58.85395	353.07619	0.02484
55815.19204	6.06366	58.85482	823.86115	0.01632
55815.65178	3.20557	58.85482	411.93014	0.01947
55825.57891	6.81791	176.53680	588.47386	0.02193
55828.40004	24.12872	176.55408	1588.86576	0.05481
55832.00784	67.89115	1118.09894	4413.55046	0.03464
55842.95719	3.41716	58.85395	353.07187	0.01880
55846.62150	7.68861	117.69840	588.47731	0.02595
55848.41960	5.73742	117.68976	529.63200	0.02068
55852.56067	20.40242	353.08829	1235.78006	0.05653
55862.50127	31.43598	647.31053	1765.39910	0.03707
55874.87472	17.49964	176.52557	1118.09462	0.04550
55878.24750	3.98561	176.54285	411.92237	0.01816
55880.92556	26.30278	176.53421	1412.32723	0.06571
55881.21230	4.94509	176.53421	411.93965	0.02558
55881.32536	9.92092	176.53507	823.85251	0.02456
55884.23091	6.25840	235.37952	765.00806	0.01940
55886.83678	10.71779	58.84445	823.85338	0.03534
55886.96755	22.22971	294.24125	1647.69811	0.02492
55888.44757	6.25139	117.69840	588.45658	0.02182
55891.30271	73.14961	470.77546	2883.48422	0.07367
55896.11193	7.12551	117.69840	706.15584	0.02458
55911.04562	4.48567	235.38038	294.24298	0.02266
55913.35318	4.19466	117.69840	294.22570	0.01940
55913.69850	16.36581	353.07965	1412.31946	0.02380
55918.65009	31.09451	117.69926	1294.63142	0.08420
55919.97075	6.28820	176.53594	588.47990	0.01913
55920.43049	30.97705	411.92669	1647.71280	0.04837
55921.79746	16.13419	176.54458	765.00720	0.04360
55921.93640	5.16064	235.38125	411.94397	0.02153
55922.14755	4.60511	176.53680	647.32522	0.01316
55925.62593	4.94213	176.54544	470.77286	0.02649
55929.51435	8.85268	117.70013	823.85597	0.02607

TABLE 3
THE OPEA MODEL PARAMETERS BY USING THE LEAST-SQUARES METHOD.

Parameter	Values	95% Confidence Intervals
Y_0	0.027 ± 0.054	-0.081 to 0.135
<i>Plateau</i>	1.951 ± 0.069	1.813 to 2.089
K	0.0007 ± 0.0001	0.0006 to 0.0008
τ	1462.9	1232.6 to 1799.1
<i>Half – life</i>	1014	854.4 to 1247.1
<i>Span</i>	1.924 ± 0.062	1.800 to 2.048
Goodness of Fit	Method	Values
R^2		0.9186
$p - value$	(D’Agostino-Pearson)	0.0011
$p - value$	(Shapiro-Wilk)	0.0009
$p - value$	(Kolmogorov Smirnov)	0.0009